Environmental Science & Technology

pubs.acs.org/est

Article

Compound Climate and Infrastructure Events: How Electrical Grid Failure Alters Heat Wave Risk

Brian Stone, Jr.,* Evan Mallen, Mayuri Rajput, Carina J. Gronlund, Ashley M. Broadbent, E. Scott Krayenhoff, Godfried Augenbroe, Marie S. O'Neill, and Matei Georgescu

Cite This: https://doi.org/10.1021/acs.est.1c00024

Read Online

ACCESS | Metrics & More | Article Recommendations

ABSTRACT: The potential for critical infrastructure failures during extreme weather events is rising. Major electrical grid failure or "blackout" events in the United States, those with a duration of at least 1 h and impacting 50,000 or more utility customers, increased by more than 60% over the most recent 5 year reporting period. When such blackout events coincide in time with heat wave conditions, population exposures to extreme heat both outside and within buildings can reach dangerously high levels as mechanical air conditioning systems become inoperable. Here, we combine the Weather Research and Forecasting regional climate model with an advanced building energy model to simulate building-interior temperatures in response to concurrent heat wave and blackout conditions for more than 2.8 million residents across Atlanta, Georgia; Detroit, Michigan; and Phoenix, Arizona. Study results find simulated compound heat wave and grid failure events of recent intensity and duration to expose between 68 and 100% of the urban population to an elevated risk of heat exhaustion and/or heat stroke.

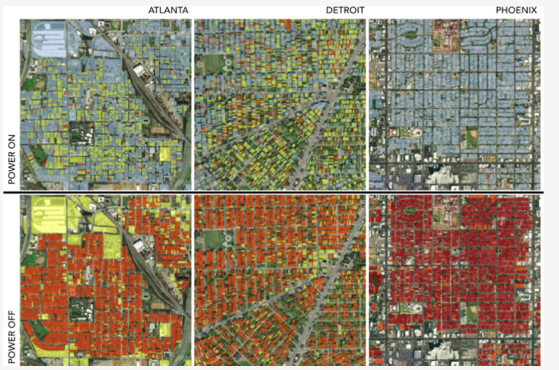

KEYWORDS: *blackout events, compound climate event, building energy model, heat wave, air conditioning systems*

1. INTRODUCTION

The potential for compound climate events is rising. The concept of compound events has been proposed for the concurrence of two climate-related phenomena that enhance societal risk, such as the outbreak of wildfires under drought conditions.[1−3] More recently, evidence of a different class of compound events—involving climatic and non-climatic stressors—is increasingly apparent, including the disruption of electricity generation and transmission under conditions of extreme heat. The annual number of major electrical grid failure or "blackout" events in the United States—those with a duration of at least 1 h and impacting 50,000 or more utility customers—increased by more than 60% over the most recent 5 year reporting period (Figure 1), with an average of 46% of these blackout events occurring between May and September, when heat risk is elevated.[4] When such blackout events coincide in time with heat wave conditions, as has occurred recently in response to wildfires and electrical grids overtaxed by high demand,[5] population exposures to extreme heat both outside and within buildings can reach dangerously high levels as mechanical air conditioning systems become inoperable.

Recent work finds the annual mortality from heat-related illness in the United States to well surpass that of any other class of extreme weather, with heat exposure contributing to an estimated 12,000 deaths each year.[6] Continued warming with climate change is expected to increase heat-related illness and mortality substantially by mid-century, independent of the compounded risk of electrical grid failures concurrent in time with hot weather.[6−11] While a rising trend in the frequency of both heat waves[12] and blackouts is elevating the potential for such compound climate and infrastructure failure events, the population health risk associated with these events, and how such risk is distributed across sub-populations, is largely unknown.[13]

In this study, we estimate the risk of extreme heat exposure to the urban populations of three major U.S. cities during a simulated compound climate and infrastructure failure event. Atlanta, Georgia; Detroit, Michigan; and Phoenix, Arizona, were selected as cases for this study due to their varying land development patterns and to the diverse climatic conditions of the Midwest, Southeast, and Southwest climate regions, in which a third of the total U.S. population resides.[14] We combine the Advanced Research version of the Weather

Received: January 4, 2021
Revised: April 10, 2021
Accepted: April 16, 2021

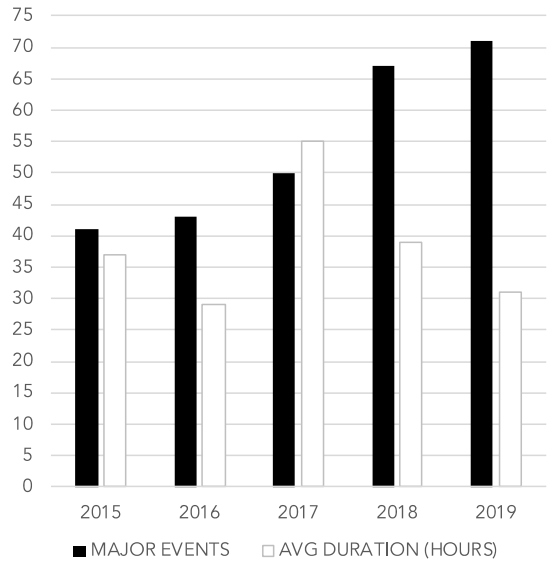

Figure 1. Total number of major electrical grid failure events and average event duration (hours) for U.S. power utilities (2015−2019).[4]

Research and Forecasting (WRF) regional climate model with a finite element approach to advanced building energy modeling (BEM) to simulate building-interior temperatures in response to heat wave conditions within 800,000 residential buildings across the three cities. Model runs focus on historical heat wave events and estimate building-interior heat index values with and without simulated electrical grid failure scenarios similar in duration to recent events impacting more than 1 million utility customers. We further make use of a novel air conditioning prevalence model[15] to estimate building-interior temperature and humidity during periods of electrical grid operability. Simulation results find a pronounced increase in the risk of heat exhaustion and heat stroke under blackout conditions and suggest significant disparities in heat exposure by building type and region.

2. MATERIALS AND METHODS

2.1. Regional Climate Model. Regional climatic conditions during a historical heat wave event were simulated with the WRF (WRF-ARW) system.[16] The WRF simulations made use of the building effect parameterization (BEP) multi-layer urban canopy model.[17] Importantly, the BEP scheme resolves meteorological variables at "street-level," meaning that the cooling impacts of interventions are captured at this level, unlike most urbanized regional climate model simulations.[18] High-resolution (1 km^2 grid spacing for the innermost domain) two-way coupled WRF-ARW + BEP (hereafter WRF) simulations were performed using a nested grid configuration, enabling the downscaling of the large-scale synoptic flow from the coarsest outer grids to the finest inner grids across the Atlanta, Detroit, and Phoenix regions. We made use of the Integrated Climate and Land Use Scenarios (ICLUS) data set for 2010,[19] available from the U.S. Environmental Protection Agency for the conterminous United States, to represent the contemporary urban landscape. ICLUS classes were mapped to the WRF domain, ranging from a rural/exurban designation to high-intensity/commercial development, using an approach similar to a recent hydroclimatic examination of urban expansion impacts.[20,21] For a full description of the WRF model setup used in this study, please refer to Broadbent et al.[18] Simulations were conducted in parallel on the high-performance computing cluster at Arizona State University. We utilized 112 processors for each simulation, with each experiment taking 48 h to complete and producing approximately 200 GB of data.

To drive our extreme heat simulations, we identified and ranked extreme heat wave events in recent history across Atlanta, Detroit, and Phoenix. Historical heat wave events were identified in each city as periods of five or more consecutive days where the 97.5th percentile daily average air temperature over the period 1980−2009 was exceeded. We selected the first or second most intense of these heat wave events in each city, prioritizing those of longest duration. The specific heat wave periods identified were August 14−18, 1995 (Atlanta); June 15−19, 1994 (Detroit); and July 20−24, 2006 (Phoenix).

In the WRF simulations, we have estimated anthropogenic heat for all sources in the lowest two atmospheric model levels at diurnal maximum rates of 10, 20, and 40 W m^{-2} for low-, medium-, and high-density urban areas.[22,23] This approach follows a widely used method for incorporation of anthropogenic heat in the single-layer urban canopy model of WRF. The profiles we have used are consistent with recently developed diurnally varying city-aggregated, warm season anthropogenic heating profiles for the three study cities.[24] In our simulations, we assume equivalent anthropogenic heating for all three cities. Although there is anthropogenic heating variability between the three cities, the similarity in diurnal behavior and overall magnitude is assumed to have a negligible impact on simulated temperatures.[24]

To assess the accuracy of WRF simulations, model output was compared to meteorological observations of air temperature from the National Climatic Data Center (NCDC) for Atlanta and Detroit, and from the Maricopa County Air Quality Department (MCAQ), the Arizona Meteorological Network (AZMET), and the MesoWest Database for Phoenix, all of which contain hourly observations of air temperature for the heat wave case studies. The monthly and daily evolution of WRF-simulated 2 m temperatures corresponded well to the observations in all three cities. The root-mean-square error of simulated air temperature at urban sites was 2.2, 2.4, and 2.6 °C for Phoenix, Atlanta, and Detroit, respectively. Simulations from Phoenix showed that WRF has a small warm bias during the day and a minor cool bias during the night.[18] In general, WRF's cool nighttime bias is stronger than the warm daytime bias. In Atlanta and Detroit, the diurnal range of temperature change was well simulated with no systematic biases.

2.2. Building Energy Model. To simulate indoor heat exposures, we made use of a finite element modeling (FEM) approach for building performance simulations inside different types of single and multi-family residential structures across the three cities.[25−27] The FEM approach modifies the widely used US Department of Energy EnergyPlus model (version 8.6)[28] to more fully represent building-interior climate conditions and to allow for numerous building prototype and ambient weather conditions to be run simultaneously. The FEM discretizes the building fabric and internal zones as a mesh of nodes and elements, where the nodes represent state variables (temperatures) and the elements represent modes of heat transfer. This model is handcrafted in MATLAB for each prototype to increase the robustness of the large number of simulations that are required for each WRF grid cell and building prototype combination. Preliminary FEM runs driven by the same building prototype, ambient conditions, and occupant behavior

https://doi.org/10.1021/acs.est.1c00024
Environ. Sci. Technol. XXXX, XXX, XXX−XXX

were found to differ from EnergyPlus output within 1 °C or less.

A single warm-up simulation cycle of three full years was run to obtain the initial temperatures of all the nodes for each prototype with typical meteorological year data. This warm-up process ensures that the temperatures of all surfaces are at equilibrium before the core simulation starts and concludes upon the commencement of the historical heat wave period. Beyond this time step, the output from WRF for each grid cell takes over the weather control and each prototype is simulated for the microclimate of that grid. This process is repeated for each 1 km^2 WRF grid cell in each city, and hourly temperatures for all residential structures are obtained for the full period of simulation. The BEM simulations utilized eight processors, required approximately 1 month of processing time for each city, and produced about 18 GB of data.

For this analysis, we simulated interior temperatures in buildings representative of typical residential structures across the three study cities. The residential structure types for which building-interior climates were simulated included one-story, single-family houses, two-story, single-family houses, and multi-story apartment buildings. The standard model prototypes for each of these building types were obtained from the US Department of Energy's EnergyPlus whole building simulation model and are constructed based on parameters from the USDOE Building Energy Codes Program.[29] Model prototype parameters, including building age, size, construction materials, and insulation values, were constructed to reflect the local residential building stock in Atlanta, Detroit, and Phoenix. In response to building inventory data, our approach makes use of higher thermal mass construction with lower insulation values for older buildings that fail to meet the 2006 International Energy Conservation Code.

Each residential structure in Atlanta, Detroit, and Phoenix was classified into one of these three standard building prototypes with the aid of parcel tax data reporting the number of stories and the number of housing units per structure. For each structure type, interior temperatures in a single, ground-level (non-basement) room were simulated. Our simulations assume that building windows are open for ventilation only if doing so would reduce indoor temperatures.

We simulate a blackout event duration comparable to recent U.S. historical events impacting populations of 1 million or more residents during a 5-month warm season (May–September). The US Energy Information Administration reports major electrical failure events for all US power utilities in the Electric Power Monthly report.[4] Based on these reports over the period of 2015–2019, the most recent 5-year period for which complete major electrical disturbance event data are available, there was a total of 272 blackout events of 1 h or more in duration and impacting 50,000 or more customers (Figure 1). We find an annual average of 54 major blackouts a year during this period, a trend that is increasing over recent decades.[30] From this data set, we identified all such major events occurring during the warm season period, when heat wave events are most probable, and impacting 1 million customers or more. The median duration of the four such events occurring during this period was 118 h. Based on this analysis, we simulate a 5-day (120 h) blackout event concurrent with historical heat wave conditions in each city.

To simulate the blackout events in the BEM, we assume that all power is lost across the full municipal area of each city at 12:00 am LST on the first of the five hottest consecutive days (based on maximum ambient temperature) of each historical heat wave and not restored for a period of 120 h. Driven by the ambient conditions provided by WRF, the BEM was run for the one-story, single-family, two-story, single-family, and multi-family apartment structures in every 1 km^2 climate model grid cell in which these structures are found and in response to two mechanical air conditioning scenarios: 100% operational AC and 0% operational AC.

2.3. Air Conditioning Prevalence Model. The Atlanta, Detroit, and Phoenix parcel attribute data sets did not consistently report information on the presence of mechanical air conditioning systems. Therefore, indoor air conditioning was modeled using an approach developed by Gronlund and Berrocal.[15] Through this approach, a regression model was developed using nationwide American Housing Survey data from 2003 to 2017, including the presence of central and window-unit air conditioning, home value, owner-occupied status, housing age, housing structure type (single vs multi-family), and metropolitan area cooling degree days. Using a predicted probability threshold of 0.5 to assign the absence versus presence of air conditioning, the out-of-sample predicted probabilities indicated overall model accuracies of 84 and 82% for central and window-unit air conditioning, respectively. For this study, home value, owner-occupied status, housing age, and housing structure type from the parcel tax records were used with metropolitan area cooling degree days to estimate the probability of central air conditioning, window-unit air conditioning, or no air conditioning system for each parcel across the three cities. Our approach does not directly capture the presence of evaporative cooling systems, which are commonly used as secondary cooling systems in Phoenix.[36]

2.4. Heat Index Computations. Ambient and building-interior model output was converted to heat index values through the following equation from Rothfusz[31]

$$\begin{aligned}\text{Heat index} = {} & -42.38 + 2.049T + 10.14\text{RH} \\ & - (0.2248T \times \text{RH}) - 0.006838T^2 \\ & - 0.05482\text{RH}^2 + (0.001229T^2 \times \text{RH}) \\ & + (0.0008528T \times \text{RH}^2) \\ & - (0.00000199T^2 \times \text{RH}^2)\end{aligned}$$

where T = ambient temperature in °F and RH = relative humidity.

If RH is less than 13% and T is between 80 and 112 °F, the following adjustment was subtracted from the heat index calculation

$$\text{Low RH adjustment} = \frac{13 - \text{RH}}{4} \times \sqrt{\frac{17 - |T - 95|}{17}}$$

If RH is greater than 85% and T is between 80 and 87 °F, the following adjustment was added to the heat index calculation

$$\text{High RH adjustment} = \frac{\text{RH} - 85}{10} \times \frac{87 - T}{5}$$

3. RESULTS AND DISCUSSION

3.1. Residential Heat Exposure Risk under Heat Wave Conditions. To assess heat exposure risk, we adopt the U.S. National Weather Service (NWS) heat index classification

https://doi.org/10.1021/acs.est.1c00024
Environ. Sci. Technol. XXXX, XXX, XXX−XXX

framework and estimate the building-interior heat index values from BEM simulations in all residential structures of the three study cities. The NWS heat index is based on a mathematical model developed by Steadman[32] and is responsive to dry-bulb temperature and RH (as detailed above). Building-interior climates are categorized into one of the five NWS heat index categories based on the average daily high heat index values during the historical heat wave periods (Figure 2).

HEAT INDEX CLASS	EXPOSURE RISK
NO RISK (< 27°C)	NONE
CAUTION (27 - 32°C)	FATIGUE
EXTREME CAUTION (32 - 41°C)	HEAT EXHAUSTION POSSIBLE, HEAT STROKE POSSIBLE
DANGER (41 - 54°C)	HEAT EXHAUSTION LIKELY, HEAT STROKE POSSIBLE
EXTREME DANGER (> 54°C)	HEAT STROKE LIKELY

Figure 2. U.S. National Weather Service heat index classification framework.[33]

Under normal electrical grid operating conditions, potentially hazardous indoor heat exposure is limited to residential structures lacking continuous mechanical air conditioning. Figure 3 maps the distribution of 5-day average maximum heat index classes for building interiors in sample residential zones of Atlanta, Detroit, and Phoenix under heat wave (top panel) and concurrent heat wave and blackout conditions (bottom panel).

Fewer than 1% of all residential structures in Phoenix are estimated to lack central air conditioning, while 6 and 47% of structures in Atlanta and Detroit, respectively, are estimated to have no or only partial access (window units) to mechanical air conditioning. On average, structures with no access to air conditioning exhibit building-interior temperatures between 8 and 16 °C higher than those with central air conditioning systems. For households lacking central air conditioning across the three cities, an average of 12% exhibit building-interior heat index values falling within the Caution category, 3% in the Extreme Caution category, and <1% in the Danger category (Phoenix only). Overall, we estimate that residents of more than 20,000 single and multi-family structures across the three cities are at risk of heat exhaustion or heat stroke under heat wave conditions and with a fully operational electrical grid.

3.2. Residential Heat Exposure Risk under Concurrent Heat Wave and Blackout Conditions. To estimate heat exposures during a compound climate and electrical grid failure event, BEM simulations were run for the same multi-day historical heat wave in each study city but with mechanical air conditioning systems assumed to be inoperable for all residential structures. Under blackout conditions, simulated building-interior heat exposures increase precipitously in residential structures equipped with central air conditioning systems. Figure 4 presents the range of 5-day average maximum building-interior heat index values by building type and city. Simulated results find heat exposures to be greatest in one-story, single-family houses across the three cities, ranging from an average of 33.5 °C in Detroit to 41.5 °C in Phoenix. The average heat index values are almost 4 °C lower in apartment buildings across the three cities, suggesting significant exposure disparities by housing type. BEM results show that shared walls between units, which are not exposed to

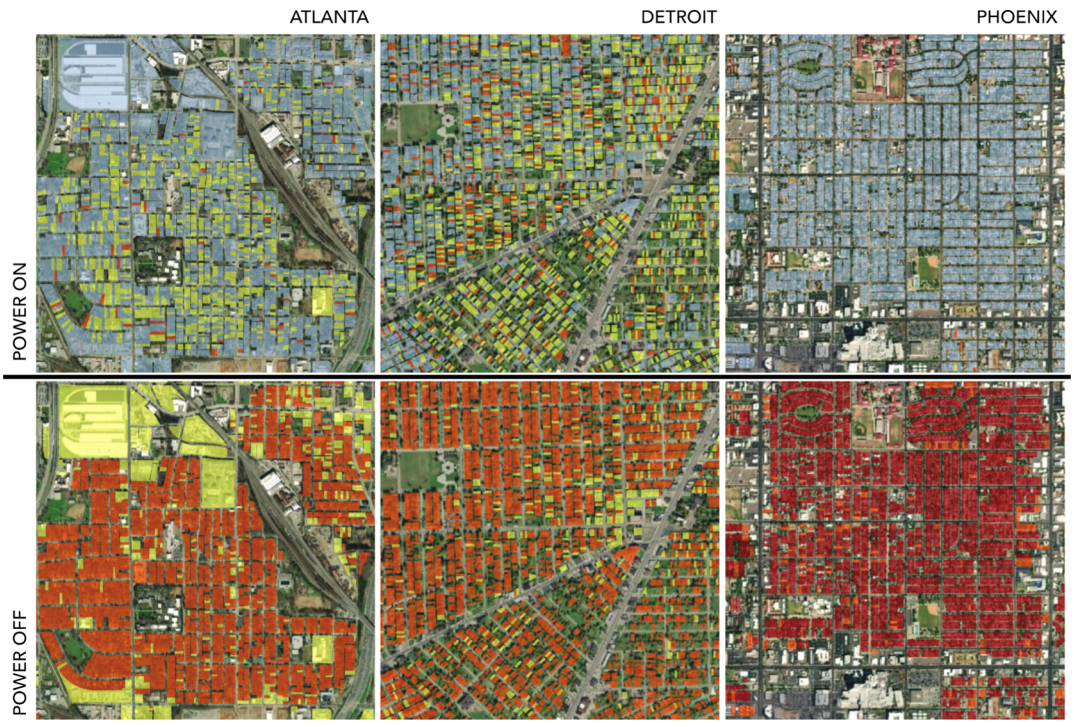

Figure 3. Example building-interior heat index classes for 5-day average maximum heat index values under historic heat wave conditions and in response to normal electrical grid operation (power on) and electrical grid failure scenarios (power off). Heat index classes as follows: No Risk (blue), Caution (yellow), Extreme Caution (orange), Danger (red).

https://doi.org/10.1021/acs.est.1c00024
Environ. Sci. Technol. XXXX, XXX, XXX−XXX

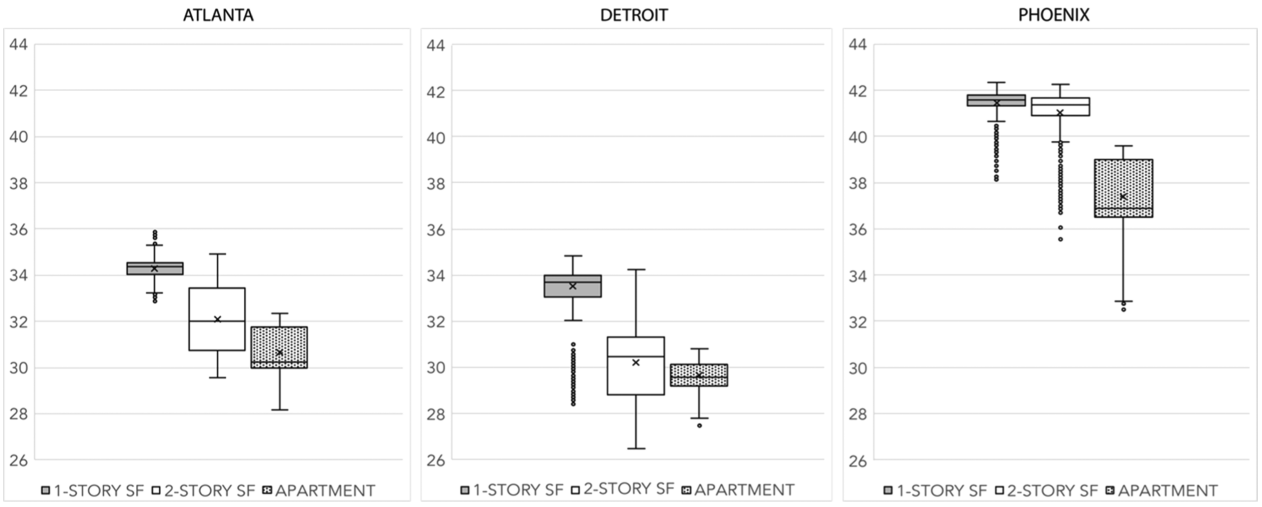

Figure 4. Boxplots for 5-day average maximum building-interior heat index values (°C) during a concurrent heat wave and electrical grid failure event. Mean values denoted with "*X*" and outliers included.

solar radiation, a larger interior air volume (increasing heat capacity), and higher average building insulation values in multifamily buildings dampen the rate at which individual units within these buildings warm following a power outage relative to single-family building types. Of the three residential structure types considered, one-story, single-family homes are found to have the lowest insulation values across each city, reducing the thermal inertia of these buildings and increasing the rate at which these structures warm during daylight hours.

In addition to building structure type, urban heat island (UHI) intensity is also found to elevate building-interior heat exposures. Figure 5 reports the average difference in building-interior maximum heat index values between the highest and lowest quintiles of ambient heat index values within each city (an indicator of UHI intensity) alongside the average difference in building-interior heat exposures between 1-story, single-family structures and apartment buildings, the warmest and coolest building types. Characterized as a UHI and housing type exposure "penalty," these results show the exposure variability associated with residential structure type to well exceed the exposure variability associated with geographic location within each city. On average, the additional heat exposure experienced in one-story, single-family structures relative to apartment buildings is 3.9 °C, while residence within the hottest zones of the city resulted in an additional building-interior heat exposure of 0.3 °C when averaged across the three cities.

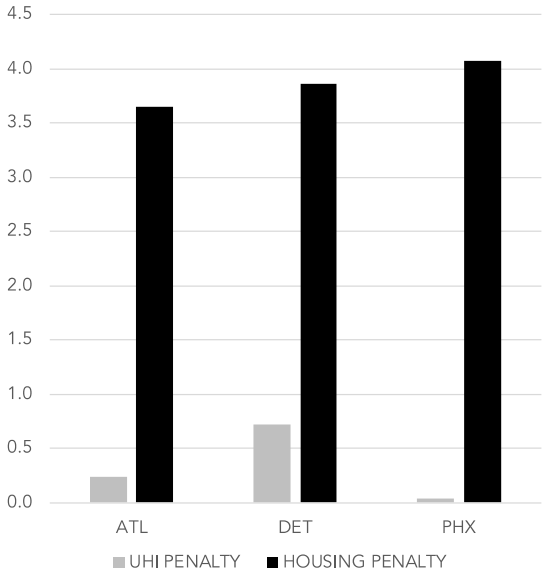

Figure 5. Differences in average 5-day maximum building-interior heat index values (°C) between the top and bottom quintiles of ambient heat index values for all structure types ("UHI penalty") and between the one-story, single-family and apartment structure types citywide ("housing penalty").

For most residential structures, higher building-interior heat index values result in a shift to a higher category of heat risk. All residential structures across the three study cities exhibit heat exposures associated with potential adverse health outcomes under simulated blackout conditions (Figure 6). In Atlanta and Detroit, approximately 30% of all structures fall into the lowest category of heat risk (Caution) while approximately 70% experience heat exposures in the Extreme Caution risk class.

A shift in heat risk is most pronounced in Phoenix, where average daily maximum heat index values were found to be approximately 43 °C outdoors and 40 °C within residential structures. Given the wide prevalence of mechanical air conditioning in Phoenix, more than 99% of the population would be expected to experience a shift in building-interior heat exposures from No Risk to the Extreme Caution or Danger categories. Prior research suggests that such an intense increase in thermal exposure over a short period of time could place Phoenix residents at a greater risk of adverse health outcomes than residents of Atlanta and Detroit, where the shift in temperatures is less dramatic and, in the instance of Detroit, AC prevalence is much lower. Temperature-related health impacts tend to be greater when exposure changes more rapidly than the human body can acclimatize, which likely explains why heat waves occurring early in the year or in cooler climates often have greater health impacts than those occurring later in the warm season.[34,35]

3.3. Compound Event Preparedness. To assess the heat exposure risk of a compound climate and electrical grid failure event, we employ widely used and validated regional climate and BEM tools to simulate outdoor and indoor climates for

https://doi.org/10.1021/acs.est.1c00024
Environ. Sci. Technol. XXXX, XXX, XXX−XXX

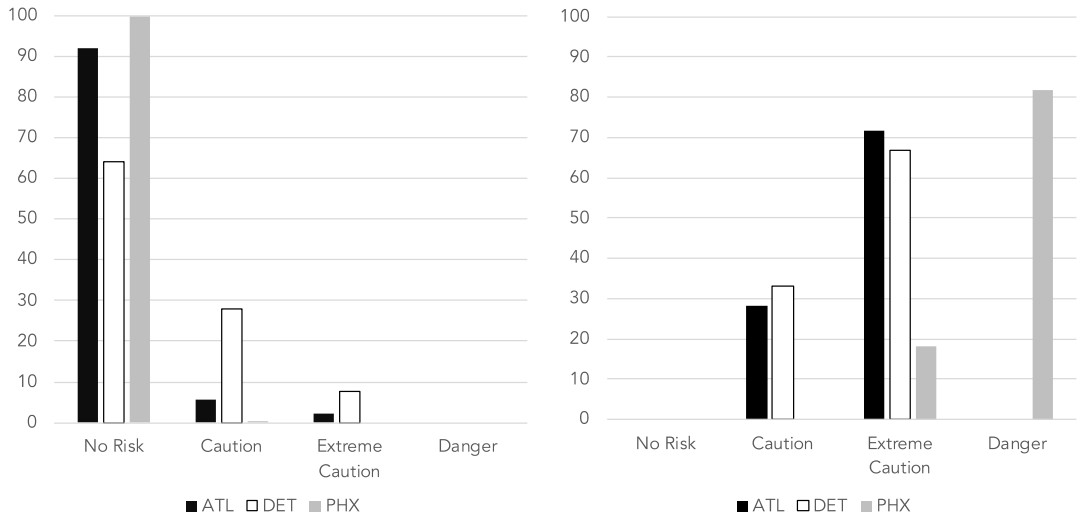

Figure 6. Percent (%) of residential structures categorized by heat index class during a simulated historical heat wave event (left panel) and a simulated concurrent heat wave and electrical grid failure event (right panel).

over 800,000 residential structures across Atlanta, Detroit, and Phoenix. The total population potentially at risk of heat-related morbidity or mortality from such an event would be in excess of 350,000 in Atlanta, 450,000 in Detroit and 1,660,000 in Phoenix. We further find tens of thousands of residents (>60,000) across the three cities to be at risk of heat illness under heat wave conditions with a fully operational electrical grid due to a lack of access to mechanical air conditioning. Given the diversity of regional climates considered, reflecting both humid and arid environments at differing latitudes, and our focus on standard housing types found in all U.S. cities, we conclude that a similar proportion of the population of any large US city (~70−100%) may be at risk of adverse health outcomes from a prolonged heat wave and blackout event as simulated herein.

While our approach enables an assessment building-interior heat exposures resulting from a compound climate and infrastructure event at the parcel level, we are not able to directly estimate population health outcomes due to a lack of information on population characteristics (e.g., age and baseline health) at the level of the individual household, as well to the unavailability of health impact functions responsive to building-interior climates. An additional limitation of our study design is the lack of historical blackout data at the parcel or district level that would support variable power supply and interior heat exposure outcomes within each city. As such district level data on the duration of blackout events is not made publicly available by local power utilities, we assume city-wide blackout events for all parcels over a full 5-day period concurrent with historical heat wave conditions. Our focus on three standard residential structures excludes manufactured housing, which accounts for 5% or less of all housing structures in each city and is less well insulated for interior thermal regulation.[36,48] We further rely on a small number of standard building prototypes to represent thermal exposures across a large and diverse set of residential structures and microclimates across the three cities. Future work by the author team will address these limitations.

None of the three cities included in our study has developed an emergency response plan to manage a compound climate event associated with widespread power outages under heat wave conditions. While each city has designated a set of public cooling centers for extreme heat emergencies, the size and number of such facilities—18 in Phoenix, 12 in Detroit, and 5 in Atlanta—would accommodate no more than 1−2% of the urban population during a concurrent heat wave and blackout event.[37−41] None of the three cities' cooling center plans requires back-up power generating capacity to ensure continued operation of mechanical cooling systems under blackout conditions.

Based on our findings, a concurrent heat wave and blackout event would require a far more extensive network of emergency cooling centers than is presently established in each city, with mandated back-up power generation. Strategies for enhanced electrical grid resilience citywide include the replacement of overhead electrical transmission lines with subsurface networks, an increased capacity for decentralized (e.g., rooftop photovoltaic) electricity generation, and an adaptation of infrastructure planning models and protocols to anticipate unprecedented climate extremes.[42] More robust heat wave warning systems, based on climate indicators more closely associated with human heat physiology, such as the regular measurement and reporting of wet-bulb globe temperatures, may be more protective of health than the NWS heat index framework most commonly used today.[43]

Coupled with enhanced electrical grid resilience is the need for urban heat management strategies designed to lessen the intensity of heat wave exposures in urban areas.[44] An extensive literature now quantifies the potential for city-wide enhancements in surface albedo and/or vegetative cover to moderate the UHI effect,[21,44,45] which should lessen building-interior exposures for households lacking mechanical cooling. Recent work by the author team focused on the same historical heat wave events in Atlanta, Detroit, and Phoenix as modeled herein finds the extensive use of cool roofs to lower maximum ambient temperatures by between 1 and 1.5 °C.[18] Other recent work has found each one percent increase in urban tree canopy to be associated with a reduction in temperatures of 0.14 and 0.2 °C in arid and humid climates, respectively.[46,47]

We find evidence of important disparities across the three cities related to household adaptive capacity for coping with extreme heat. While access to continuous mechanical air conditioning is widely recognized as a fundamental adaptive strategy for managing heat risk,[15] our analysis suggests that the

https://doi.org/10.1021/acs.est.1c00024
Environ. Sci. Technol. XXXX, XXX, XXX−XXX

size of the residential structure is an additional risk factor for households lacking mechanical cooling or during periods of grid inoperability concurrent with hot weather. Lack of access to central air conditioning in the home and residence in single-story structures and the structure type most conducive to elevated building-interior heat exposures are both more common for low-income households than for high-income households. On average across the three study cities, households falling into the lowest quintile of median household income are about 20% more likely to lack central air conditioning than households in the highest quintile of median household income.[36] Likewise, the lowest income households are about 20% more likely to reside in single-story structures, on average, than the highest income households.[36] This disparity in adaptive capacity for lower income households results in a greater heat risk burden for this population, during periods of both grid operability and inoperability.

This work finds simulated compound climate and infrastructure events to pose a significant health threat to the population of three major U.S. cities and a growing risk for the U.S. population as a whole. In concert with rapidly rising warm season temperatures in major cities globally, the frequency of major electrical grid system failures is rising in the United States.[30] We find simulated blackout events concurrent with heat waves of historical intensity in three large cities spanning a range of climate zones to expose residents of between 68 and 100% of all residential structures to adverse health outcomes, including heat exhaustion and heat stroke. Lowering the risk of such compound climate and infrastructure events will require significant investments in regional electrical grid resilience, urban heat management programs, and heat wave emergency response systems.

AUTHOR INFORMATION

Corresponding Author

Brian Stone, Jr. − *School of City and Regional Planning, Georgia Institute of Technology, Atlanta, Georgia 30332, United States;* orcid.org/0000-0002-2418-0486; Phone: 404 894 6488; Email: stone@gatech.edu

Authors

Evan Mallen − *School of City and Regional Planning, Georgia Institute of Technology, Atlanta, Georgia 30332, United States*

Mayuri Rajput − *School of Architecture, Georgia Institute of Technology, Atlanta, Georgia 30332, United States*

Carina J. Gronlund − *School of Public Health, University of Michigan, Ann Arbor, Michigan 48109, United States*

Ashley M. Broadbent − *School of Geographical Sciences and Urban Planning, Arizona State University, Tempe, Arizona 85287, United States*

E. Scott Krayenhoff − *School of Environmental Sciences, University of Guelph, Guelph, Ontario N1G 2W1, Canada*

Godfried Augenbroe − *School of Architecture, Georgia Institute of Technology, Atlanta, Georgia 30332, United States*

Marie S. O'Neill − *School of Public Health, University of Michigan, Ann Arbor, Michigan 48109, United States*

Matei Georgescu − *School of Geographical Sciences and Urban Planning, Arizona State University, Tempe, Arizona 85287, United States*

Complete contact information is available at: https://pubs.acs.org/10.1021/acs.est.1c00024

Notes

The authors declare no competing financial interest.

ACKNOWLEDGMENTS

This material is based on the work supported by the National Science Foundation under grant number 1520803 and by the National Institute of Environmental Health Sciences under grant numbers P30ES017885 and R00ES026198. Any opinions, findings, and conclusions, or recommendations, expressed in this material are those of the authors and do not necessarily reflect the views of the National Science Foundation or the National Institute of Environmental Health Sciences.

REFERENCES

(1) Intergovernmental Panel on Climate Change (IPCC). *Managing the Risks of Extreme Events and Disasters to Advance Climate Change Adaptation. A Special Report of Working Groups I and II of the Intergovernmental Panel on Climate Change*; Field, C. B., Barros, V., Stocker, T. F., Qin, D., Dokken, D. J., Ebi, K. L., Mastrandrea, M. D., Mach, K. J., Plattner, G.-K., Allen, S. K., Tignor, M., Midgley, P. M., Eds.; Cambridge University Press: Cambridge, UK, and New York, NY, USA, 2012; pp 582.

(2) Leonard, M.; Westra, S.; Phatak, A.; Lambert, M.; van den Hurk, B.; McInnes, K.; Risbey, J.; Schuster, S.; Jakob, D.; Stafford-Smith, M. A compound event framework for understanding extreme impacts. *Wiley Interdiscip. Rev.: Clim. Change* **2014**, *5*, 113−128.

(3) Zscheischler, J.; Westra, S.; van den Hurk, B. J. J. M.; Seneviratne, S. I.; Ward, P. J.; Pitman, A.; AghaKouchak, A.; Bresch, D. N.; Leonard, M.; Wahl, T.; Zhang, X. Future climate risk from compound events. *Nat. Clim. Change* **2018**, *8*, 469−477.

(4) US Energy Information Administration (USEIA). Electric Power Monthly. 2016−2020, https://www.eia.gov/electricity/monthly/ (accessed online Aug 1, 2020).

(5) Clark, S. S.; Chester, M. V.; Seager, T. P.; Eisenberg, D. A. The vulnerability of interdependent urban infrastructure systems to climate change: Could Phoenix experience a Katrina of extreme heat? *Sustainable Resilient Infrastruct.* **2019**, *4*, 21−35.

(6) Shindell, D.; Zhang, Y.; Scott, M.; Ru, M.; Stark, K.; Ebi, K. L. The Effects of Heat Exposure on Human Mortality Throughout the United States. *GeoHealth* **2020**, *4*, No. e2019GH000234.

(7) Voorhees, A. S.; Fann, N.; Fulcher, C.; Dolwick, P.; Hubbell, B.; Bierwagen, B.; Morefield, P. Climate change-related temperature impacts on warm season heat mortality: A proof-of-concept methodology using BenMAP. *Environ. Sci. Technol.* **2011**, *45*, 1450−1457.

(8) Bobb, J. F.; Peng, R. D.; Bell, M. L.; Dominici, F. Heat-related mortality and adaptation to heat in the United States. *Environ. Health Perspect.* **2014**, *122*, 811−816.

(9) Honda, Y.; Kondo, M.; McGregor, G.; Kim, H.; Guo, Y.-L.; Hijioka, Y.; Yoshikawa, M.; Oka, K.; Takano, S.; Hales, S.; Kovats, R. S. Heat-related mortality risk model for climate change impact projection. *Environ. Health Prev. Med.* **2014**, *19*, 56−63.

(10) Mills, D.; Schwartz, J.; Lee, M.; Sarofim, M.; Jones, R.; Lawson, M.; Duckworth, M.; Deck, L. Climate change impacts on extreme temperature mortality in select metropolitan areas in the United States. *Clim. Change* **2015**, *131*, 83−95.

(11) Schwartz, J. D.; Lee, M.; Kinney, P.; Yang, S.; Mills, D.; Sarofim, M.; Jones, R.; Streeter, R.; Juliana, A.; Peers, J.; Horton, R. Projections of temperature-attributable premature deaths in 209 U.S. cities using a cluster-based Poisson approach. *Environ. Health* **2015**, *14*, 85.

(12) Habeeb, D.; Vargo, J.; Stone, B. Rising heat wave trends in large US cities. *Nat. Hazards* **2015**, *76*, 1651−1665.

(13) Raymond, C.; Horton, R. M.; Zscheischler, J.; Martius, O.; AghaKouchak, A.; Balch, J.; Bowen, S. G.; Camargo, S. J.; Hess, J.; Kornhuber, K.; Oppenheimer, M.; Ruane, A. C.; Wahl, T.; White, K.

Understanding and managing connected extreme events. *Nat. Clim. Change* **2020**, *10*, 611−621.
(14) Karl, T.; Koss, W. *Regional and National Monthly, Seasonal, and Annual Temperature Weighted by Area, 1895−1983*; Historical Climatology Series 4-3; National Climatic Data Center: Asheville, NC, 1984; pp 38.
(15) Gronlund, C. J.; Berrocal, V. J. Modeling and comparing central and room air conditioning ownership and cold-season in-home thermal comfort using the American Housing Survey. *J. Exposure Sci. Environ. Epidemiol.* **2020**, *30*, 814−823.
(16) Skamarock, W. C.; Klemp, J. B.; Dudhia, J.; Gill, D. O.; Barker, D. M.; Duda, M. G.; Huang, X. Y.; Wang, W.; Powers, J. G. *A Description of the Advanced Research WRF Version 3 B*; National Center for Atmospheric Research: CO, 2008; pp 1−105.
(17) Martilli, A.; Clappier, A.; Rotach, M. W. An urban surface exchange parameterisation for mesoscale models. *Boundary-Layer Meteorol.* **2002**, *104*, 261−304.
(18) Broadbent, A. M.; Krayenhoff, E. S.; Georgescu, M. Efficacy of cool roofs at reducing pedestrian-level air temperature during projected 21st century heatwaves in Atlanta, Detroit, and Phoenix (USA). *Environ. Res. Lett.* **2020**, *15*, 084007.
(19) Bierwagen, B. G.; Theobald, D. M.; Pyke, C. R.; Choate, A.; Groth, P.; Thomas, J. V.; Morefield, P. National housing and impervious surface scenarios for integrated climate impact assessments. *Proc. Natl. Acad. Sci. U. S. A.* **2010**, *107*, 20887−20892.
(20) Krayenhoff, E. S.; Moustaoui, M.; Broadbent, A. M.; Gupta, V.; Georgescu, M. Diurnal interaction between urban expansion, climate change and adaptation in US cities. *Nat. Clim. Change* **2018**, *8*, 1097−1103.
(21) Georgescu, M.; Morefield, P. E.; Bierwagen, B. G.; Weaver, C. P. Urban adaptation can roll back warming of emerging megapolitan regions. *Proc. Natl. Acad. Sci. U.S.A.* **2014**, *111*, 2909−2914.
(22) Chow, W. T. L.; Salamanca, F.; Georgescu, M.; Mahalov, A.; Milne, J. M.; Ruddell, B. L. A multi-method and multi-scale approach for estimating city-wide anthropogenic heat fluxes. *Atmos. Environ.* **2014**, *99*, 64−76.
(23) Sailor, D. J.; Lu, L. A top−down methodology for developing diurnal and seasonal anthropogenic heating profiles for urban areas. *Atmos. Environ.* **2004**, *38*, 2737−2748.
(24) Sailor, D. J.; Georgescu, M.; Milne, J. M.; Hart, M. A. Development of a national anthropogenic heating database with an extrapolation for international cities. *Atmos. Environ.* **2015**, *118*, 7−18.
(25) Rajput, M.; Augenbroe, F. Heat stress in residential buildings as a result of deficient HVAC systems. *Proceedings of the International Building Performance Simulation Association Conference*, Rome, Italy, 2019; pp 2482−2490.
(26) Li, B.; Duffield, C. F.; Hutchinson, G. L. Simplified Finite Element Modelling of multi-story buildings: The Use of equivalent cubes. *Electron. J. Struct. Eng.* **2008**, *8*, 40−45.
(27) Augenbroe, G.; Brown, J.; Heo, Y.; Kim, S.; Li, Z.; McManus, S.; Fei, Z. Lessons from an advanced building simulation course. *Proceedings of the International Building Performance Simulation Association Conference*, Berkeley, CA, 2008; pp 261−268.
(28) Crawley, D. B.; Lawrie, L. K.; Pedersen, C. O.; Winkelmann, F. C. EnergyPlus: Energy Simulation Program. *ASHRAE J.* **2000**, *42*, 49−56.
(29) US Department of Energy (USDOE). Residential Prototype Building Models, Building Codes Energy Program. 2017, https://www.energycodes.gov/development/residential/iecc_models (accessed on Sep 1, 2018).
(30) Hines, P.; Apt, J.; Talukdar, S. Large blackouts in North America: Historical trends and policy implications. *Energy Policy* **2009**, *37*, 5249−5259.
(31) Rothfusz, L. *The Heat Index Equation*. Technical Attachment SR 90-23; US National Weather Service, 1990.
(32) Steadman, R. G. The assessment of sultriness. Part I: A temperature-humidity index based on human physiology and clothing science. *J. Appl. Meteorol.* **1979**, *18*, 861−873.
(33) National Weather Service, US National Oceanic and Atmospheric Administration. Heat Index Chart. 2021, https://www.weather.gov/ffc/hichart (accessed online Oct 28, 2020).
(34) Anderson, B. G.; Bell, M. L. Weather-related mortality: how heat, cold, and heat waves affect mortality in the United States. *Epidemiology* **2009**, *20*, 205−213.
(35) Curriero, F. C.; Heiner, K. S.; Samet, J. M.; Zeger, S. L.; Strug, L.; Patz, J. A. Temperature and Mortality in 11 Cities of the Eastern United States. *Am. J. Epidemiol.* **2002**, *155*, 80−87.
(36) US Census Bureau, American Housing Survey. American Housing Survey Table Creator. 2019, https://www.census.gov/programs-surveys/ahs/data/interactive/ahstablecreator.html (accessed online March 24, 2021).
(37) City of Atlanta. ATL311 Non-Emergency Services. 2020, https://www.atl311.com/wp-content/uploads/2015/06/City-of-Atlanta-Cooling-Centers.pdf (accessed online Oct 28, 2020).
(38) City of Detroit. Cooling Centers. 2020, https://detroitmi.gov/departments/homeland-security-emergency-management-detroit/shelters-warming-and-cooling-centers/cooling-centers (accessed online Sept 16, 2020).
(39) Fulton County. Fulton County Senior Facilities Serve as Cooling Centers on Weekdays during Extreme Heat. 2020, http://fultoncountygov.blogspot.com/2016/07/fulton-county-senior-facilities-serve.html (accessed online Oct 28, 2020).
(40) Maricopa County. Cooling Stations and Water Donation Sites. 2020, https://www.maricopa.gov/2461/Cooling-Stations-Water-Donation (accessed online Oct 28, 2020).
(41) Wayne County. Cooling centers in Wayne County are open to keep you safe during heat advisory. 2020, https://www.waynecounty.com/elected/executive/cooling-centers-in-wayne-county-are-open-to-keep-you.aspx (accessed online Oct 28, 2020).
(42) Brockway, A. M.; Dunn, L. N. Weather adaptation: Grid infrastructure planning in a changing climate. *Clim. Risk Manage.* **2020**, *30*, 100256.
(43) Cheng, Y.-T.; Lung, S.-C. C.; Hwang, J.-S. New approach to identifying proper thresholds for a heat warning system using health risk increments. *Environ. Res.* **2019**, *170*, 282−292.
(44) Stone, B.; Lanza, K.; Mallen, E.; Vargo, J.; Russell, A. Urban Heat Management in Louisville, Kentucky: A Framework for Climate Adaptation Planning. *J. Plann. Educ. Res.* **2019**, 0739456X1987921.
(45) Krayenhoff, E. S.; Jiang, T.; Christen, A.; Martilli, A.; Oke, T. R.; Bailey, B. N.; Nazarian, N.; Voogt, J. A.; Giometto, M. G.; Stastny, A.; Crawford, B. R. A multi-layer urban canopy meteorological model with trees (BEP-Tree): Street tree impacts on pedestrian-level climate. *Urban Clim.* **2020**, *32*, 100590.
(46) Middel, A.; Chhetri, N.; Quay, R. Urban forestry and cool roofs: Assessment of heat mitigation strategies in Phoenix residential neighborhoods. *Urban For. Urban Green.* **2015**, *14*, 178−186.
(47) Skelhorn, C.; Lindley, S.; Levermore, G. The impact of vegetation types on air and surface temperatures in a temperate city: A fine scale assessment in Manchester, UK. *Landsc. Urban Plann.* **2014**, *121*, 129−140.
(48) Gabbe, C. J.; Pierce, G. Extreme Heat Vulnerability of Subsidized Housing Residents in California. *Hous. Policy Debate* **2020**, *30*, 843−860.

https://doi.org/10.1021/acs.est.1c00024
Environ. Sci. Technol. XXXX, XXX, XXX−XXX